Large-scale integrated focal plane array for two-dimensional scanning

Lei Yu,[1,2] Yifan Xin,[1,2] Pengfei Wang,[1,2,*] Guangzhen Luo,[1,2] Pengfei Ma,[1,2] Zheng Wang,[1,2] Licheng Chen,[1,2] Yibo Yang,[1,2] Yejin Zhang,[1,2] and Jiaoqing Pan[1,2,]**

[1]Key Laboratory of Semiconductor Materials Science, Institute of Semiconductors, Chinese Academy of Sciences, Beijing 100083, China
[2]Center of Materials Science and Optoelectronics Engineering, University of Chinese Academy of Sciences, Beijing 100049, China
*[*]pfwang15@semi.ac.cn; **jqpan@semi.ac.cn*

Abstract: The focal plane array is regarded as a promising solution for LiDAR. In this work, we present an ultra-large-scale focal plane array featuring 1024 antennas and 2113 micro-rings with a FoV of 85.7° × 29.5°.

1. Introduction

LiDAR is widely used to acquire environmental information in fields such as assisted driving, intelligent robotics, and aerospace [1–4]. However, the existing architectures relying on mechanical components suffer from longevity-related flaws. Consequently, several all-solid-state beam scanning schemes have been proposed. Among them, the lens-assisted focal plane array (FPA), which operates by directing the input light to a designated antenna using an optical switch array, is considered a promising solution [5–8]. The primary challenge currently impeding the extensive adoption of FPA is the quantity of point clouds. In particular, the reported results predominantly utilize the Mach-Zehnder-Interferometer (MZI)-based optical switch array, whose substantial size severely hampers the number of antennas. To address this issue, some alternatives have been proposed. For instance, we previously demonstrated a two-dimensional (2D) beam steering FPA chip based on a micro-ring switch array [9], which offers greater compactness compared to the MZI-based FPA. Simultaneously, this structure demands extremely low operational complexity and overall power consumption since only one optical switch works at a time.

In this paper, we demonstrate an ultra-large-scale densely integrated FPA based on the micro-ring switch array, consisting of 1024 antennas and 2113 micro-rings. A large field of view (FoV) measuring 85.7° × 29.5° has been achieved through the application of the FoV splicing technology and the antenna multiplexing technology. In addition, the FPA chip is scalable, and showcases the limitless potentials of silicon photonics.

2. Design and Manufacturing

The FPA can be segmented into four components: input coupler, micro-ring-based optical switch array, antenna array, and assisted lens, while schematic illustrations of the first three components can be found in Fig. 1 (a). During working, the input light is initially routed to a designated antenna through the optical switch array and subsequently emitted into free space. Meanwhile, a lens positioned above the chip collimates and redirects the emitted beam, resulting in the one-dimensional (1D) quasi-continuous scanning in the transverse direction (φ). If we adjust the wavelength of the input light, the 1D continuous scanning in the longitudinal direction (θ) can be achieved. The following equation provides the steering angle of FPA in the θ-direction [10], λ represents the vacuum wavelength of the incident light, n_{eff} denotes the effective index of the waveguides, and n_{ct} corresponds to the refractive index of the medium through which the emitted beam propagates. It can be found that simply increasing the wavelength tuning range is not sufficient to achieve a large scanning range (VFoV). To tackle this challenge, we employ the FoV splicing technology and the antenna multiplexing technology. In particular, the FoV splicing technology refers to the design of N antennas for end-to-end far-field splicing, as depicted in Fig. 1(b), which enables the VFoV to expand N times. Meanwhile, the antenna multiplexing technology enables the realization of two symmetrical VFoV by routing the input light to both ends of the antenna.

$$sin\theta = \frac{\Lambda n_{eff} - \lambda}{\Lambda n_{ct}} \tag{1}$$

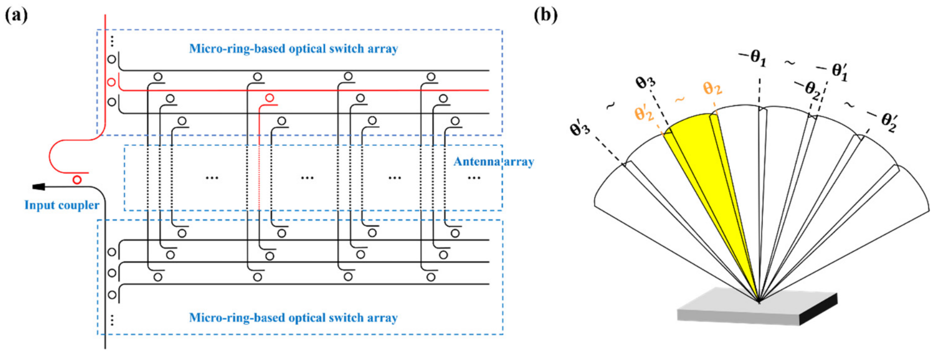

Fig. 1. (a) Design diagram of the FPA chip. (b) Schematic of the FoV splicing technology and the antenna multiplexing technology.

3. Characterization

The proposed FPA chip was fabricated by Advanced Micro Foundry (AMF) using the Si_3N_4 on SOI platform, enabling us to achieve high-power input, low phase noise antennas, and low-loss cross waveguides. The fabricated chip, as shown in Fig. 2, comprises of 1024 antennas and 2113 micro-rings. In this system, one micro-ring is employed for antenna multiplexing, while the remaining micro-rings (33 × 32 × 2) are utilized for channel switching. To increase the effective apertures, we adopted the antenna incorporating the Si_3N_4 perturbations on the Si waveguide. Meanwhile, eight types of antennas have been designed by adjusting the perturbation parameters to achieve the FoV splicing, which means that the FPA is equivalent to a 128-line (1024/8) LiDAR. Additionally, our designed FPA operates within the C-band, imposing significantly reduced laser requirements compared to the optical phased array, which necessitates tuning beyond 100 nm [11,12].

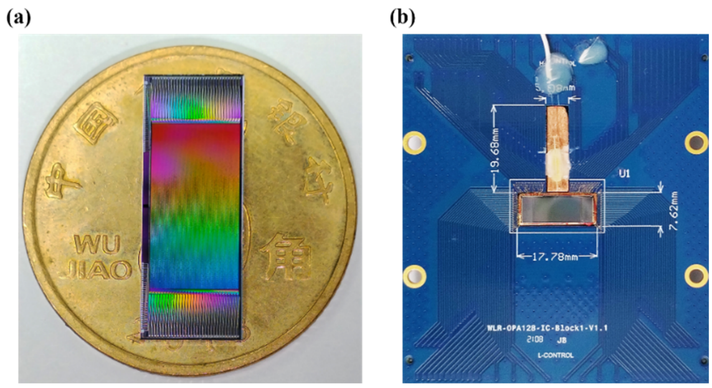

Fig. 2. (a) Photography of the fabricated chip. (b) Photography of the fabricated chip after packing.

In this work, a 10 mm focal length lens was utilized as the collimator, and the beams were characterized at wavelengths of 1530 nm, 1540 nm, and 1550 nm. Fig. 3 displays the 17 lines chosen from the 128 lines in the φ-direction. The utilization of the FoV splicing technology and the antenna multiplexing technology enabled the FPA to achieve a large FoV measuring 85.7° × 29.5°. The denser light spots near θ = 0° are the result of the slight overlap of two FoVs formed by the antenna multiplexing technology, and this design is implemented to prevent blind spots. In future work, we will demonstrate more scanning lines of this FPA chip, and beams at other wavelengths.

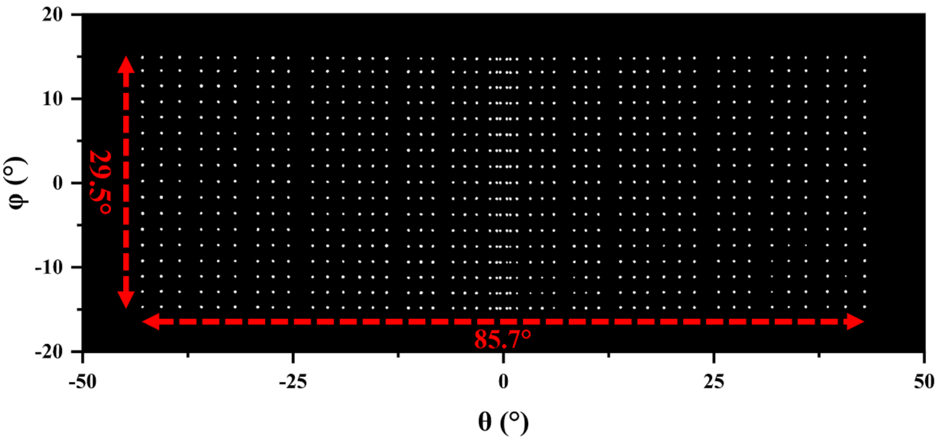

Fig. 3. Beams of FPA at 1530 nm, 1540 nm, and 1550 nm (17 lines selected from 128 lines).

4. Conclusion

In this paper, we demonstrate an ultra-large-scale densely integrated FPA, which consists of 1024 antennas and 2113 micro-rings. The FPA exhibits minimal operational complexity and overall power consumption as it uses two or three micro-rings simultaneously. By utilizing the FoV splicing technology and the antenna multiplexing technology, we realized a broad FoV of 85.7° × 29.5°. In future work, we will demonstrate more scanning lines of this FPA chip, along with beams at other wavelengths. In summary, our design effectively enhances the integration and the VFoV of FPA. We believe that this scalable structure will drive the advancement of FPA.

Acknowledgements

This work was supported in part by the National Key R&D Program of China (2022YFB2804503), and in part by the National Natural Science Foundation of China (62105324, 62090053, and 61934007). The authors would like to thank VANJEE Technology for their support in the area of circuits.

References

1. K. Sayyah, R. Sarkissian, P. Patterson, B. Huang, O. Efimov, D. Kim, K. Elliott, L. Yang, and D. Hammon, "Fully Integrated FMCW LiDAR Optical Engine on a Single Silicon Chip," J. Lightwave Technol. **40**, 2763–2772 (2022).
2. C. V. Poulton, M. J. Byrd, P. Russo, B. Moss, O. Shatrovoy, M. Khandaker, and M. R. Watts, "Coherent LiDAR With an 8,192-Element Optical Phased Array and Driving Laser," IEEE J. Select. Topics Quantum Electron. 1–8 (2022).
3. P. Munoz, D. Pastor, L. A. Bru, G. M. Cabanes, J. Benitez, D. Goodwill, and E. Bernier, "Scalable Switched Slab Coupler Based Optical Phased Array on Silicon Nitride," IEEE J. Select. Topics Quantum Electron. **28**, 1–16 (2022).
4. L. Yu, P. Wang, P. Ma, L. Cui, Z. Wang, Y. Yang, Y. Zhang, and J. Pan, "Two-dimensional beam scanning of passive optical phased array based on silicon nitride delay line," J. Lightwave Technol. **41**, 2756–2764 (2023).
5. C. Rogers, A. Y. Piggott, D. J. Thomson, R. F. Wiser, I. E. Opris, S. A. Fortune, A. J. Compston, A. Gondarenko, F. Meng, X. Chen, G. T. Reed, and R. Nicolaescu, "A universal 3D imaging sensor on a silicon photonics platform," Nature **590**, 256–261 (2021).
6. T. Tamanuki, H. Ito, and T. Baba, "Thermo-Optic Beam Scanner Employing Silicon Photonic Crystal Slow-Light Waveguides," J. Lightwave Technol. **39**, 904–911 (2021).
7. X. Zhang, K. Kwon, J. Henriksson, J. Luo, and M. C. Wu, "A large-scale microelectromechanical-systems-based silicon photonics LiDAR," Nature **603**, 253–258 (2022).
8. C. Li, K. Wu, X. Cao, G. Zhang, T. Li, Z. Deng, M. Chang, Y. Wang, X. Li, and J. Chen, "Monolithic coherent LABS lidar based on an integrated transceiver array," Opt. Lett. **47**, 2907–2910 (2022).
9. L. Cui, P. Wang, Q. Zhao, P. Ma, Z. Wang, L. Yu, Y. Yang, Y. Zhang, and J. Pan, "Two-dimensional scanning of silicon-based focal plane array with field-of-view splicing technology," Opt. Express **31**, 1464 (2023).
10. C.-P. Hsu, B. Li, B. Solano-Rivas, A. R. Gohil, P. H. Chan, A. D. Moore, and V. Donzella, "A Review and Perspective on Optical Phased Array for Automotive LiDAR," IEEE J. Select. Topics Quantum Electron. **27**, 1–16 (2021).
11. P. Ginel-Moreno, A. Sánchez-Postigo, J. de-Oliva-Rubio, A. Hadij-ElHouati, W. N. Ye, J. G. Wangüemert-Pérez, Í. Molina-Fernández, J. H. Schmid, P. Cheben, and A. Ortega-Moñux, "Millimeter-long metamaterial surface-emitting antenna in the silicon photonics platform," Opt. Lett. **46**, 3733 (2021).
12. Y. Liu and H. Hu, "Silicon optical phased array with a 180-degree field of view for 2D optical beam steering," Optica **9**, 903 (2022).